



Published in final edited form as:

*Breast Cancer Res Treat.* 2013 April ; 138(3): 761–772. doi:10.1007/s10549-013-2501-6.

## Genomic and Expression Analysis of Microdissected Inflammatory Breast Cancer

Wendy A Woodward<sup>1,8</sup>, Savitri Krishnamurthy<sup>2,8</sup>, Hideko Yamauchi<sup>3</sup>, Randa El-Zein<sup>4,8</sup>, Dai Ogura<sup>5</sup>, Eri Kitadai<sup>3</sup>, Shin-ichiro Niwa<sup>5</sup>, Massimo Cristofanilli<sup>7,8</sup>, Peter Vermeulen<sup>10</sup>, Luc Dirix<sup>10</sup>, Patrice Viens<sup>9</sup>, Steve van Laere<sup>10,11</sup>, François Bertucci<sup>9</sup>, James M. Reuben<sup>6,8</sup>, and Naoto T. Ueno<sup>7,8</sup>

<sup>1</sup>Department of Radiation Oncology, The University of Texas MD Anderson Cancer Center, Houston, TX

<sup>2</sup>Department of Pathology, The University of Texas MD Anderson Cancer Center, Houston, TX

<sup>3</sup>Department of Breast Surgery, St. Luke's International Hospital Tokyo, Japan

<sup>4</sup>Department of Epidemiology, The University of Texas MD Anderson Cancer Center, Houston, TX

<sup>5</sup>Link Genomics, Tokyo, Japan

<sup>6</sup>Department of Hematopathology, The University of Texas MD Anderson Cancer Center, Houston, TX

<sup>7</sup>Department of Breast Medical Oncology, The University of Texas MD Anderson Cancer Center, Houston, TX

<sup>8</sup>Morgan Welch Inflammatory Breast Cancer Research Program and Clinic, The University of Texas MD Anderson Cancer Center, Houston, TX

The Department of Medical Oncology, Institut Paoli-Calmettes, Marseille, France

<sup>10</sup>Translational Cancer Research Unit, Sint-Augustinus Hospital, Antwerp, Belgium

<sup>11</sup>Department of Oncology, KU Leuven, Leuven, Belgium

### Abstract

**Purpose**—Inflammatory breast cancer (IBC) is a unique clinical entity characterized by rapid onset of erythema and swelling of the breast often without an obvious breast mass. Many studies have examined and compared gene expression between IBC and non-IBC (nIBC), repeatedly finding clusters associated with receptor subtype, but no consistent gene signature associated with IBC has been validated. Here we compared microdissected IBC tumor cells to microdissected nIBC tumor cells matched based on estrogen and HER-2/*neu* receptor status.

**Methods**—Gene expression analysis and comparative genomic hybridization were performed. An IBC gene set and genomic set were identified using a training set and validated on the remaining data. The IBC gene set was further tested using data from IBC consortium samples and publically available data.

**Results**—Receptor driven clusters were identified in IBC; however no IBC-specific gene signature was identified. Fifteen genes were correlated between increased genomic copy number

\*Corresponding author: Naoto T. Ueno, MD, PhD, nueno@mdanderson.org.

Conflict of Interest: The authors have no conflicts of interest to disclose.

and gene overexpression data. An expression-guided gene set upregulated in the IBC training set clustered the validation set into two clusters independent of receptor subtype but segregated only 75% of samples in each group into IBC or nIBC. In a larger consortium cohort and in published data the gene set failed to optimally enrich for IBC samples. However, this gene set had a high negative predictive value for excluding the diagnosis of IBC in publically available data (100%). An IBC enriched genomic data set accurately identified 10/16 cases in the validation data set.

**Conclusions**—Even with microdissection, no IBC-specific gene signature distinguishes IBC from nIBC. Using microdissected data, a validated gene set was identified that is associated with IBC tumor cells. IBC comparative genomic hybridization data are presented, but a validated genomic data set that identifies IBC is not demonstrated.

## Keywords

Inflammatory breast cancer; CGH; array; gene signature

## Introduction

Inflammatory Breast Cancer (IBC) is a clinically defined variant of breast cancer characterized by its rapid onset and swollen, erythematous, and edematous presentation of the breast. Pathologically IBC is associated with tumor emboli in the dermal lymphatics, and diffuse tumor infiltrate through tissue making it more difficult to image and more difficult to obtain purely tumor cells for genetic assessment. Although several studies have attempted to characterize an IBC gene signature, thus far none has been identified robustly [1–10]. One potential limitation of the published gene array studies in IBC is the inclusion of tissue samples likely to contain both tumor and stroma. Indeed, the only prior study of microdissected IBC samples found significant gene differences in the stroma rather than the tumor cells themselves [11]. Herein we described a gene array and comparative genomic hybridization based comparison of IBC and non-inflammatory breast cancer (nIBC) tumor cells based on microdissection to exclude tumor stroma and environmental contributions. The genome copy number and mRNA expression signature of IBC, nIBC, and non-cancerous breast tissue (Normal) were analyzed, and the gene profile and copy number characteristics of IBC were investigated.

## Material and Methods

Twenty IBC frozen tissue samples from core biopsies were obtained from The University of Texas MD Anderson Cancer Center, Houston, TX under IRB-approved protocol. Twenty nIBC and 5 normal breast frozen tissues from surgical specimens were obtained from St. Luke's International Hospital Tokyo, Japan under IRB-approved protocol. Inflammatory, T4D stage was assigned when the pathologic diagnosis of breast cancer based on the consensus criteria formalized in the international consensus statement by Dawood et al [12]. Specifically, the inflammatory T4d diagnosis was made in patients with clinical symptoms of breast erythema, edema and/or peau d'orange, and/or warm breast, with or without an underlying palpable mass present over at least one third of the breast for less than 6 months. Clinical symptoms in the setting of a neglected primary were not considered IBC. Pathologic evidence of tumor emboli in the dermis was not required for diagnosis. Samples were selected from a prospective tissue registry based on availability of high quality material for the study. In total, 32 core biopsies were analyzed and 20 paired samples with high quality RNA and DNA examined. The nIBC samples were matched according to the marker status of IBC on *HER2/neu* (HER2) amplification and estrogen receptor (ER) status. Samples with low DCIS component were selected to avoid DCIS influence. Marker status and DCIS component for each case are listed in Supplemental table 1.

## Genomic DNA and RNA Sample preparation

Cancer cells of tumor specimen and epithelium of normal breast specimen were collected for genomic DNA and RNA extraction. For tumor samples, 5–20 frozen sections of biopsy (16  $\mu\text{m}$  thick) were manually microdissected. Under the guidance of a pathologist, normal tissue was removed leaving > 90% tumor cells. For normal breast samples, 40–60 frozen sections of surgical specimen (16  $\mu\text{m}$  thick) were subjected to microdissection manually. Genomic DNA was extracted using the Quick Gene SP-kit DNA tissue (Fujifilm; Tokyo, Japan), and quality was characterized with Agarose gel electrophoresis. Human Female Genomic DNA (Novagen; Madison, WI, USA) was used for normal reference DNA. Total RNA was extracted using the RNeasy micro kit (Qiagen; Valencia, CA, USA), and quality was characterized with BioAnalyzer (Agilent Technologies; Waldbronn, Germany).

## Preparation of Whole Genome DNA Microarray

Whole Genome DNA Microarray was created with complete coverage of the human genome using 12310 individually amplified bacterial artificial chromosomes (BAC) clones. All BAC clones were cultured from a single colony and validated by PCR amplification using clone specific primers that were designed in-house. Extracted BAC DNAs were BstYI restricted and amplified by ligation-mediated PCR. The products were printed on glass slides with an inkjet-type spotter.

## Analysis of genome copy number – Array CGH analysis

Alu I and Rsa I-restricted genomic DNAs were labeled by random priming with Alexa555-dCTP (test DNA) and Alexa647-dCTP (reference DNA) using the BioPrime Plus ArrayCGH Indirect Genomic Labeling System (Invitrogen). Labeled test and reference DNAs were ethanol precipitated in the presence of Cot-1 DNA, redissolved in a hybridization mix, and denatured at 70°C for 10 min. After incubation at 42°C for 5 min, the mixture was applied to Whole Genome DNA Microarray (LinkGenomics) covered with a MAUI Mixer hybridization chamber (Biomicro systems). After incubation at 42°C for 48 hours, slides were washed with 2 $\times$ SSC/0.1%SDS buffer and 0.1 $\times$ SSC/0.1%SDS buffer several times. After rinsing with 0.01 $\times$ SSC buffer and air-drying, slides were scanned with a Microarray Scanner (Agilent Technologies), and analyzed with Gene-Pix Pro 4.0 imaging software (Axon Instruments; Union City, CA, USA). Normalization was performed using global-normalization methods and fold changes of genome copy number compared with normal tissue were calculated. Thresholds for gains and losses were set to 1.2 and 0.8, respectively.

## Analysis of mRNA expression – Microarray analysis

RNA samples were labeled using the Low Input Quick Amp Labeling kit (Agilent Technologies). Labeled cRNA was hybridized to an oligo-nucleotide microarray (Whole Human Genome 4 $\times$ 44K, Agilent Technologies) at 65°C for 17 hours. After washing with the Gene Expression Wash Buffer kit (Agilent Technologies) and drying, the slides were scanned with a Agilent Microarray Scanner, and analyzed with the Feature Extraction software version 9.5.1 (Agilent Technologies). Normalization was performed using global-normalization methods.

## Analysis and statistics

Data from microarray and CGH have been deposited in the public GEO database ID number XX. 1000 probes having the greatest SD were chosen for unsupervised hierarchical clustering analysis of all samples (20 IBC, 20 non-IBC, and 5 normal). Genes differentially expressed between non-IBC and IBC were determined based on T-test (non-paired) p-values < 0.001 and fold change  $\geq 2$  and gene ontology functional analysis was performed of

differentially expressed genes. Genome copy number profiles were determined using a ratio of green to red (G/R) signal of  $>1.2$  and  $<0.8$  to identify regions of gain or loss, respectively. Comparison was made between nIBC and IBC samples using Fisher's exact test ( $P < 0.01$  considered differentially expressed). Correlation of genome copy number and mRNA expression value was computed (Pearson's correlation coefficient), and genes with significant correlation ( $r \geq 0.6$ ) selected.

The overall study design of mRNA analysis for identification of IBC samples is presented in Figure 1. To identify a gene set that selected for IBC a learning set and validation approach was used. In the learning set, genes were filtered by an expression fold change  $\geq 2$  with a T-test (unpaired)  $p$ -value  $< 0.05$  ( $N = 779$ ). Then, a threshold for each gene was determined (Supplemental data file 1) which provided the minimum number of the sum of false positive and false negative genes leaving a gene set of 132 genes differentially expressed in IBC. This gene set was then confirmed in the validation set, in public data, and in a multi-institutional consortium data set. Within each sample in the learning set, each gene was scored positive or negative for IBC likeness where it was considered positive for IBC if the expression level was higher than the threshold for that gene. The IBC score of each sample was then defined as the percentage of genes for that sample that were positive for IBC: (the number of positive genes divided by the total number of genes in the set)  $\times 100$ . Therefore IBC score defines an index of IBC-likeness (Supplemental data file 1). The learning set validation approach was the performed using the IBC likeness score as well. IBC diagnostic criteria were set to 43% to separate the two groups. The same approach was then used to evaluate IBC-likeness in the validation set, the multi-institution data, and the publically available data.

The overall study design for CGH analysis for identification of IBC samples is presented in Figure 2. Analyzing the genomic data, a learning set and validation approach was used. Differentially expressed BACs were based on Fisher's exact test,  $P < 0.01$ . Fifty five BACs that were differentially gained or lost in IBC were selected and confirmed in the validation set. As in the array analysis, an IBC likeness score using the CGH data was determined in the learning set and examined in the validation set. The number of differentially expressed BACs in IBC that were present in each sample in the learning set were divided by the total number of BACs as above to determine IBC likeness. Based on the discrimination of the learning set, the IBC threshold was set at 51.8% and examined in the validation set.

## Results

### Comparison of expression profiles in the total dataset

Unsupervised hierarchical clustering analysis of all samples (IBC 20, nIBC 20, Normal 5) was performed with the 1000 most informative (highest SD) RNA probes. Three clusters were formed. Cluster A was predominantly ER positive cases (89%, 17 out of 19), cluster B was predominantly ER negative cases (63%, 12 out of 19), and cluster C included all of the normal cases (71%, 5 out of 7). IBC represented 37%, 63% and 14% of cluster A, B, and C respectively. This analysis was repeated without the normal samples revealing similar results (Supplemental data file 1). The genes with a fold change  $\geq 2$  and  $P \leq 0.001$  on non-paired T-test were considered differentially expressed between IBC and nIBC. 131 genes showed significant differential expression between IBC and nIBC (Figure 3 and Supplemental Table 2). Gene ontology analysis was performed with differentially expressed genes and revealed that the functions of gas transport, cell adhesion, and angiogenesis are activated in IBC, and response to hormone stimulus is inactivated in IBC (Table 1).

## Genomic analysis in the total data set

Across all samples, gain of 1q and 8q, and loss of 8p occurred in high frequencies in both IBC and nIBC (Figures 4 and 5). The aberrations in these regions are well known for breast cancer. Loss of 16q occurred in higher frequencies in nIBC compared to IBC. Sixty-four BACs were identified with difference in the frequency of genome copy number aberration between IBC and nIBC (Supplemental Table 3). Six regions (1p34, 1p12, 2p25, 2p21, 6p22-6p21, 9q34) had gains more frequently in IBC, and 5 regions (14q11, 14q22-14q23, 16p13-16p11, 20q13, 22q11) had gains more frequently in nIBC. Eight regions (5q13, 8p23, 8p21, 9p12, 16q12-16q13, 16q22, 17p13-17p11, 17q21) had losses more frequently in nIBC. There were no regions in which loss frequency was higher in IBC. Examining the concordance between genome copy number and gene expression data revealed 15 genes that were significantly correlated between genome copy number and mRNA expression. These were located in 6p21-22 and 20q13 and were considered candidate IBC specific genes (Table 2).

## Assessment of IBC by mRNA expression

To evaluate whether mRNA expression could be used to distinguish IBC and nIBC, 24 samples (IBC 12, nIBC 12) were used as "learning set" and the remaining 16 samples were used as validation set. 779 genes with  $\geq 2$ -fold difference and  $P < 0.05$  were selected. As described in the methods and Supplemental data file 1, a threshold was applied to lower the false negative and false positive rates leaving 132 genes in the gene set for IBC assessment. One hundred genes were up in IBC and 32 were down in IBC. Hierarchical clustering analysis of the learning set was performed with 132 genes revealing two clusters were formed that distinguish IBC from nIBC (Supplemental data file 1). ER+ cases were equally distributed between the two clusters (75%). All cases in cluster B were IBC cases and all cases in cluster A were nIBC. Subsequently, unsupervised hierarchical clustering analysis of the validation set was performed with selected genes (Figure 6a). Two clusters were formed. ER+ cases were equally distributed between clusters, and Cluster B contained 75% of IBC cases. IBC assessment was performed using the IBC score described in the methods (Figure 6b) identified in the learning set and tested in the validation set. As expected, all samples for the learning set were correctly classified. In the validation set, 2 IBC samples were judged to be nIBC with scores of 23.5 and 29.5, respectively. Two nIBC samples were judged to be IBC with scores of 56.8 and 60.6, respectively. Thus in the validation set, 12 out of 16 samples (75%) were judged correctly. The positive and negative predictive values were both 75% and the false negative and positive rates were both 25%.

The IBC assessment was further evaluated using the integrated data from 3 institutions [2, 5, 7]. Analytical data of 389 pretreatment breast tumor samples (IBC 137, nIBC 252) on Affymetrix platform (about 7,000 genes at the time of integration) were available. Data have been made available at arrayexpress ID numbers E-MTAB-1547, E-MTAB-1006 and xx. All samples were invasive adenocarcinomas. Patients with IBC were selected by strictly adhering to the consensus diagnostic criteria published by Dawood and colleagues [12]. IBC cases included non-metastatic and metastatic cases. nIBC cases included both early stage disease (two institutions) and advanced stage disease (one institution. No microdissection had been performed on these samples. Clustering analysis was conducted using 44 genes, which were in common with the 132 differential genes described earlier (Table 3, Figure 7). No cluster was enriched for IBC samples. We then assessed the prediction of IBC status using these 44 genes (Figure 8). Distribution of IBC and nIBC overlapped and could not be distinguished clearly. The negative predictive value (NPV) was 79% for all samples, 81% in Marseille samples, 74% in MDA samples, 82% in Antwerp samples. The validity of the IBC assessment method, which we considered, was further examined using two public data sets [11, 13]. Distribution of IBC and nIBC overlapped and could not be distinguished clearly

(Figure 9). However, NPV was again very high (100%) suggesting this gene set might be useful to exclude IBC in samples that were not microdissected.

### Assessment of IBC by genome copy number

We next sought to determine whether it would be possible to distinguish IBC and nIBC using genome copy number aberration. Twenty-four samples (IBC 12, nIBC 12) comprised the "learning set" and 16 samples comprised the "validation set". Fifty-five BACs were identified in the learning set ( $P < 0.01$ , Supplemental Table 4). In the learning set, IBC-likeness was computed in each sample as the number of IBC differentiated BACs divided by the total number of BACs, and this IBC score approach was evaluated (Figure 10). Two IBC samples were judged to be nIBC both with scores of 45.5. These were not the same cases misjudged by the mRNA assessment. Two nIBC samples were judged to be IBC with scores of 85.5 and 63.6. These also were not the same cases identified using the mRNA approach. Therefore, in the learning set, 20 out of 24 samples (83%) were judged correctly. The positive and negative predictive value was 83%. IBC diagnostic score threshold was set to 51.8. IBC assessment in the validation set using the IBC score calculated as described above based on the 55 BACs identified in the learning set was performed (Figure 10). A score of 51.8 or higher was judged as IBC. One IBC sample was judged to be nIBC with a score of 30.9. Five nIBC samples were judged to be IBC (scores 89.1, 85.5, 74.5, 70.9, and 63.3). Therefore in the validation set, 10 out of 16 samples (63%) were judged correctly. The positive and negative predictive values were 58% and 75%, respectively. The false negative and false positive rates were 12.5% and 62.5%, respectively.

### Conclusion

Here we provide a gene expression assessment of receptor status-matched microdissected IBC, and the first comparative genomic analysis of microdissected IBC. Consistent with prior reports [1–10], no IBC specific signature was clearly established. Nevertheless, correlation of mRNA upregulation and increased genome copy number revealed 15 genes that are correlated between these approaches clustered largely at 6p21. An IBC specific gene set was identified in microdissected samples that may identify biology specific to tumor cells and may further be useful to exclude the diagnosis of IBC. Still, the diagnosis of IBC remains a clinical diagnosis even after microdissected analysis, perhaps suggesting the role of the host and microenvironment is critical to this molecular phenotype.

While the rarity of IBC limits the prospects for large analyses of patient samples, many studies have examined gene expression signatures from IBC patients in an effort to identify a molecular determinant of this clinically variable disease [1–10]. Several issues independent of the technical considerations inherent in array based studies make the development of such an IBC discriminator challenging. The diffuse nature of IBC, often presenting without a dominant mass, makes it likely that differences in the ratio of tumor and non-tumor cells will exist in IBC vs. nIBC biopsy specimens when laser capture microdissection is not performed. In addition, it remains unclear whether the ideal comparison represents unselected nIBC patients, or stage-matched T4a-c nIBC patients. Lastly, the dominance of the basal subtype in the IBC cohort further confounds these analyses.

Bieche et al examined a larger group of IBC patients, 37, and compared the tumor gene expression to 22 stage II and III nIBC tumor samples [3]. Significantly up-regulated genes coded for transcription factors (*JUN*, *EGR1*, *JUNB*, *FOS*, *FOSB*, *MYCN*, and *SNAIL1*), growth factors (*VEGF*, *DTR/HB-EGF*, *IGFBP7*, *IL6*, *ANGPT2*, *EREG*, *CCL3/MIPIA*, and *CCL5/RANTES*), and growth factor receptors (*TBXA2R*, *TNFRSF10A/TRAILR1*, and *ROBO2*). Iwamoto et al compared gene expression analysis from 25 T4d IBC patients to 57

stage- and subtype-matched nIBC T4a-c patients [5]. Unlike the prior reports, comparing expression data from all IBC with all nIBC revealed no significant differences after adjusting for multiple testing. Further, none of the previously described IBC gene signatures effectively discriminated these samples into IBC and nIBC, potentially highlighting the inherent limitations of signatures based on small numbers as well as the heterogeneity in IBC samples as defined clinically. This was not the only study that did not find a clear signature in unsupervised analysis. Nguyen et al compared 14 IBC samples where IBC was clinically defined as rapid-onset cancer associated with erythema and skin changes, to 20 nIBC patients with stage III breast cancers, using the Affymetrix HG-U133A microarrays. Similar to the study by Iwamoto, they found no significant differences at the individual gene level but observed some differences at the gene set level [6]. Gene expression analyses indicated that IBC had higher expression of genes associated with increased metabolic rate, lipid signaling, and cell turnover relative to nIBC tumors.

In the aggregate, while all studies identify discernable differences in gene expression in IBC compared to non-IBC, these studies all failed to define an IBC-specific gene signature that can be validated across other samples. A recent collaborative study combining data from three institutions has been completed, and is being analyzed. Interestingly, the only other study to examine microdissected IBC reports differences in the stromal component of IBC rather than the tumor cells themselves[11].

Although the limitations of this study include the relatively small sample size and difference in origin of the IBC and nIBC samples that may impact the findings, these data in the context of the existing literature suggest that the IBC phenotype is not distinguishable by gene expression differences. Initial investigation of DNA hypermethylation has similarly failed to reveal a predictive signature in spite of individual differences in specific promoters [14], and while additional studies including next generation sequencing may reveal yet unappreciated genomic drivers, these data imply that differences in tumor cells may not be the distinguishing feature of IBC.

## Supplementary Material

Refer to Web version on PubMed Central for supplementary material.

## Acknowledgments

We appreciate the patients who provided samples for these studies and the Morgan Welch Inflammatory Breast Cancer Clinic and Research Program for support.

Compliance: All experiments herein comply with all federal laws in the US and Japan governing the use of human tissues and protection of human subjects.

Financial support: The National Institute of Health R01CA138239-01; The State of Texas Grant for Rare and Aggressive Cancers.

## References

1. Bertucci F, Finetti P, Rougemont J, Charafe-Jauffret E, Cervera N, Tarpin C, et al. Gene expression profiling identifies molecular subtypes of inflammatory breast cancer. *Cancer research*. 2005; 65:2170–2178. [PubMed: 15781628]
2. Bertucci F, Finetti P, Rougemont J, Charafe-Jauffret E, Nasser V, Loriod B, et al. Gene expression profiling for molecular characterization of inflammatory breast cancer and prediction of response to chemotherapy. *Cancer research*. 2004; 64:8558–8565. [PubMed: 15574762]

3. Bieche I, Lerebours F, Tozlu S, Espie M, Marty M, Lidereau R. Molecular profiling of inflammatory breast cancer: identification of a poor-prognosis gene expression signature. *Clin Cancer Res.* 2004; 10:6789–6795. [PubMed: 15501955]
4. Dressman HK, Hans C, Bild A, Olson JA, Rosen E, Marcom PK, et al. Gene expression profiles of multiple breast cancer phenotypes and response to neoadjuvant chemotherapy. *Clin Cancer Res.* 2006; 12:819–826. [PubMed: 16467094]
5. Iwamoto T, Bianchini G, Qi Y, Cristofanilli M, Lucci A, Woodward WA, et al. Different gene expressions are associated with the different molecular subtypes of inflammatory breast cancer. *Breast Cancer Res Treat.* 125:785–795. [PubMed: 21153052]
6. Nguyen DM, Sam K, Tsimelzon A, Li X, Wong H, Mohsin S, et al. Molecular heterogeneity of inflammatory breast cancer: a hyperproliferative phenotype. *Clin Cancer Res.* 2006; 12:5047–5054. [PubMed: 16951220]
7. Van Laere S, Van der Auwera I, Van den Eynden G, Van Hummelen P, van Dam P, Van Marck E, et al. Distinct molecular phenotype of inflammatory breast cancer compared to non-inflammatory breast cancer using Affymetrix-based genome-wide gene-expression analysis. *British journal of cancer.* 2007; 97:1165–1174. [PubMed: 17848951]
8. Van Laere S, Van der Auwera I, Van den Eynden GG, Fox SB, Bianchi F, Harris AL, et al. Distinct molecular signature of inflammatory breast cancer by cDNA microarray analysis. *Breast Cancer Res Treat.* 2005; 93:237–246. [PubMed: 16172796]
9. Van Laere SJ, Van den Eynden GG, Van der Auwera I, Vandenberghe M, van Dam P, Van Marck EA, et al. Identification of cell-of-origin breast tumor subtypes in inflammatory breast cancer by gene expression profiling. *Breast Cancer Res Treat.* 2006; 95:243–255. [PubMed: 16261404]
10. Van Laere SJ, Van der Auwera I, Van den Eynden GG, Elst HJ, Weyler J, Harris AL, et al. Nuclear factor-kappaB signature of inflammatory breast cancer by cDNA microarray validated by quantitative real-time reverse transcription-PCR, immunohistochemistry, and nuclear factor-kappaB DNA-binding. *Clin Cancer Res.* 2006; 12:3249–3256. [PubMed: 16740744]
11. Boersma BJ, Reimers M, Yi M, Ludwig JA, Luke BT, Stephens RM, et al. A stromal gene signature associated with inflammatory breast cancer. *International journal of cancer.* 2008; 122:1324–1332. [Research Support, N.I.H., Extramural Research Support, N.I.H., Intramural].
12. Dawood S, Merajver SD, Viens P, Vermeulen PB, Swain SM, Buchholz TA, et al. International expert panel on inflammatory breast cancer: consensus statement for standardized diagnosis and treatment. *Annals of oncology : official journal of the European Society for Medical Oncology / ESMO.* 2011; 22:515–523. [Consensus Development Conference Practice Guideline Research Support, N.I.H., Extramural Research Support, Non-U.S. Gov't]. [PubMed: 20603440]
13. Sircoulomb F, Bekhouche I, Finetti P, Adelaide J, Ben Hamida A, Bonansea J, et al. Genome profiling of ERBB2-amplified breast cancers. *BMC cancer.* 2010; 10:539. [Research Support, Non-U.S. Gov't]. [PubMed: 20932292]
14. Van der Auwera I, Bovie C, Svensson C, Limame R, Trinh XB, van Dam P, et al. Quantitative assessment of DNA hypermethylation in the inflammatory and non-inflammatory breast cancer phenotypes. *Cancer Biol Ther.* 2009; 8:2252–2259. [PubMed: 19829046]



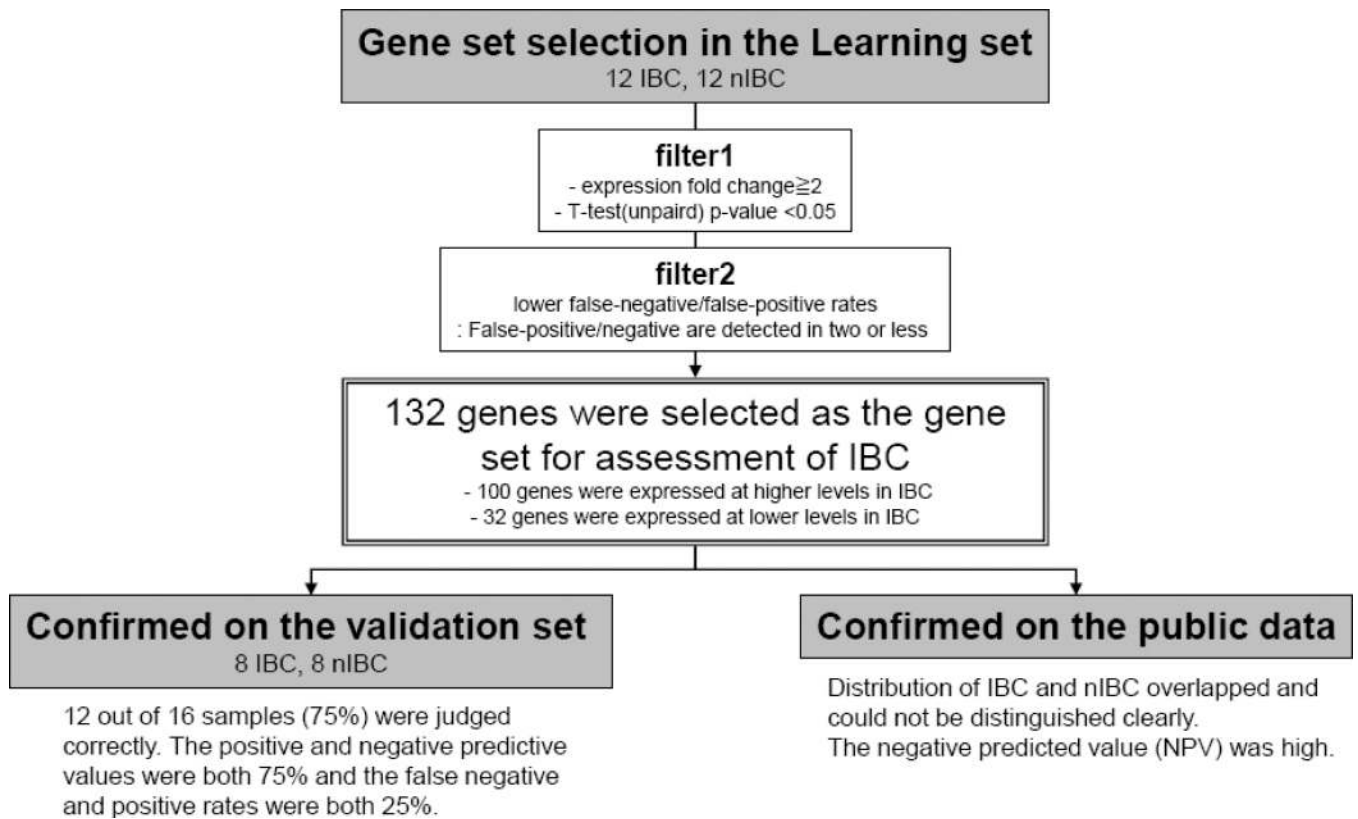


**Figure 1. Flow chart summarizing the assessment of IBC by mRNA expression**  
mRNA expression signature in a training set consisting of 24 samples (12 IBC and 12 non-IBC) was analyzed. The 132 genes were selected as the gene set for assessment of IBC. Afterwards, we confirmed on the validation set consisting of 16 samples (8 IBC and 8 non-IBC), and public data.

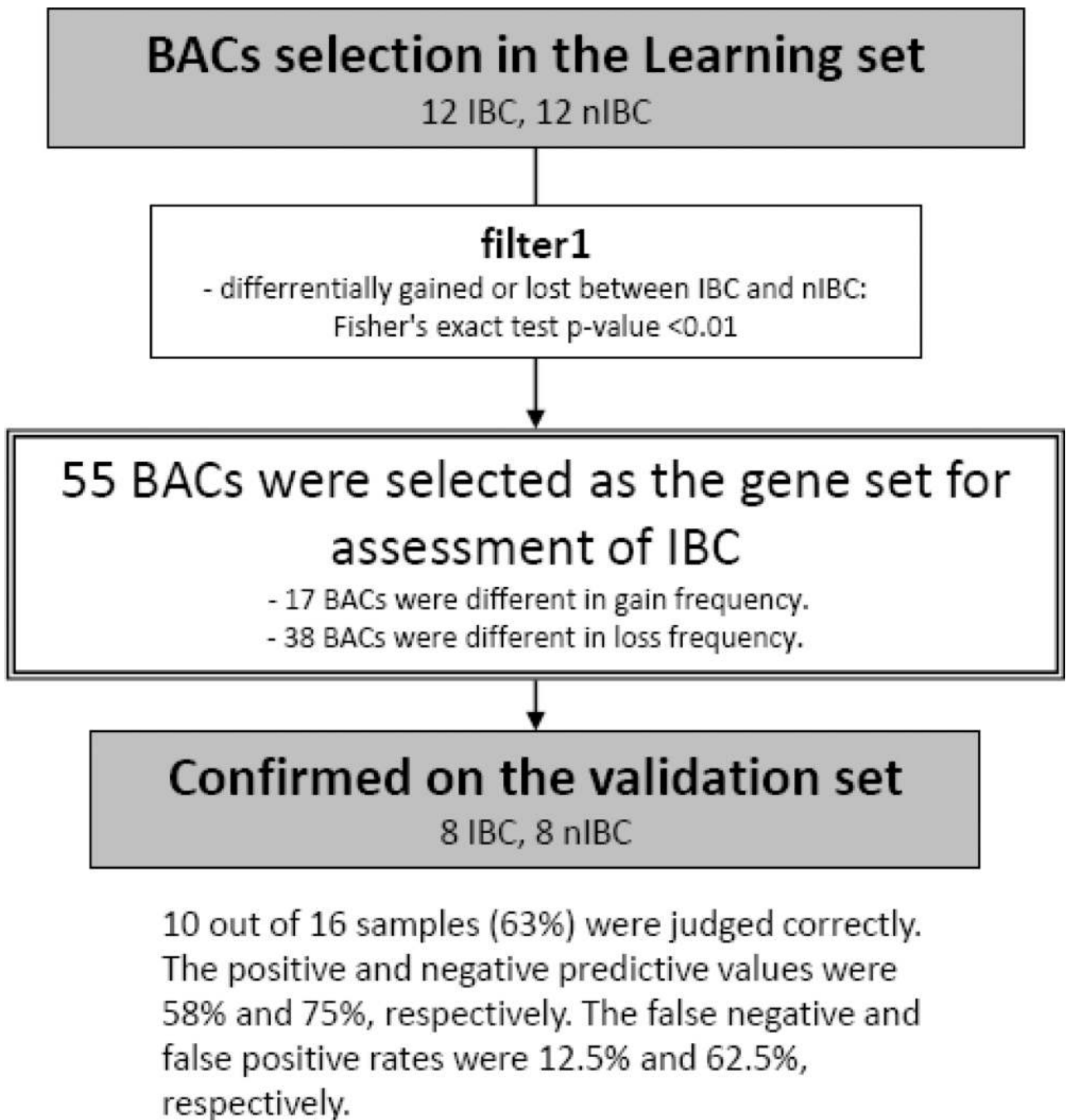


**Figure 2. Flow chart summarizing the assessment of IBC by genome copy number**  
Gain or loss frequencies in a training set consisting of 24 samples (12 IBC and 12 non-IBC) were analyzed. The 55 BACs were selected as the gene set for assessment of IBC. Afterwards, we confirmed on the validation set consisting of 16 samples (8 IBC and 8 non-IBC).

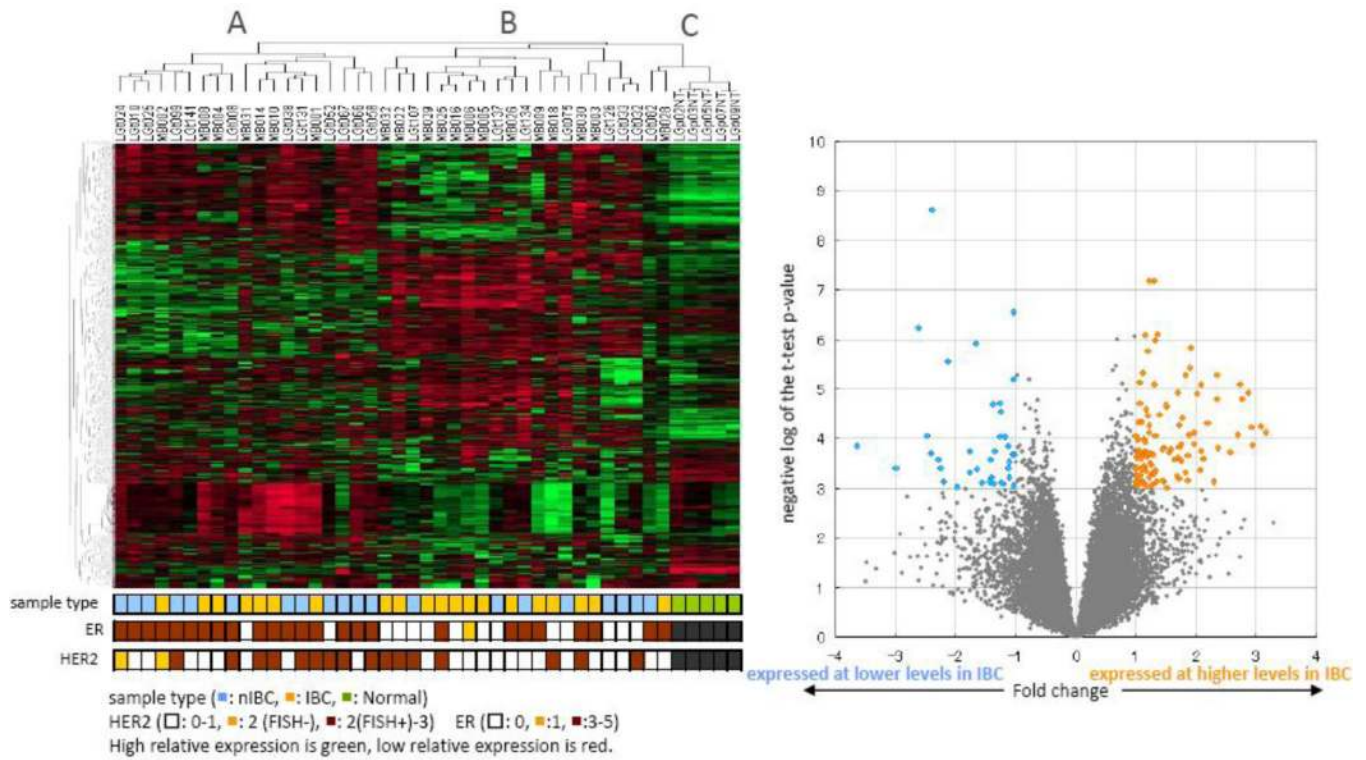


**Figure 3. Hierarchical clustering analysis**

Left, 1000 probes having the greatest SD were chosen for unsupervised hierarchical clustering analysis of 45 samples (20 IBC, 20 nIBC, 5 Normal). High relative expression is green, low relative expression is red. Sample type (IBC or nIBC or Normal) and ER/HER2 status (based on IHC) of the samples are color-coded as shown. Right, Volcano plot showing fold change (in log<sub>2</sub> space) on the x-axis and negative log of the t-test p-value on the y-axis. The orange dots represent the probes that were expressed at higher levels in the IBC group. The blue dots represent the probes that were expressed at lower levels in IBC group.

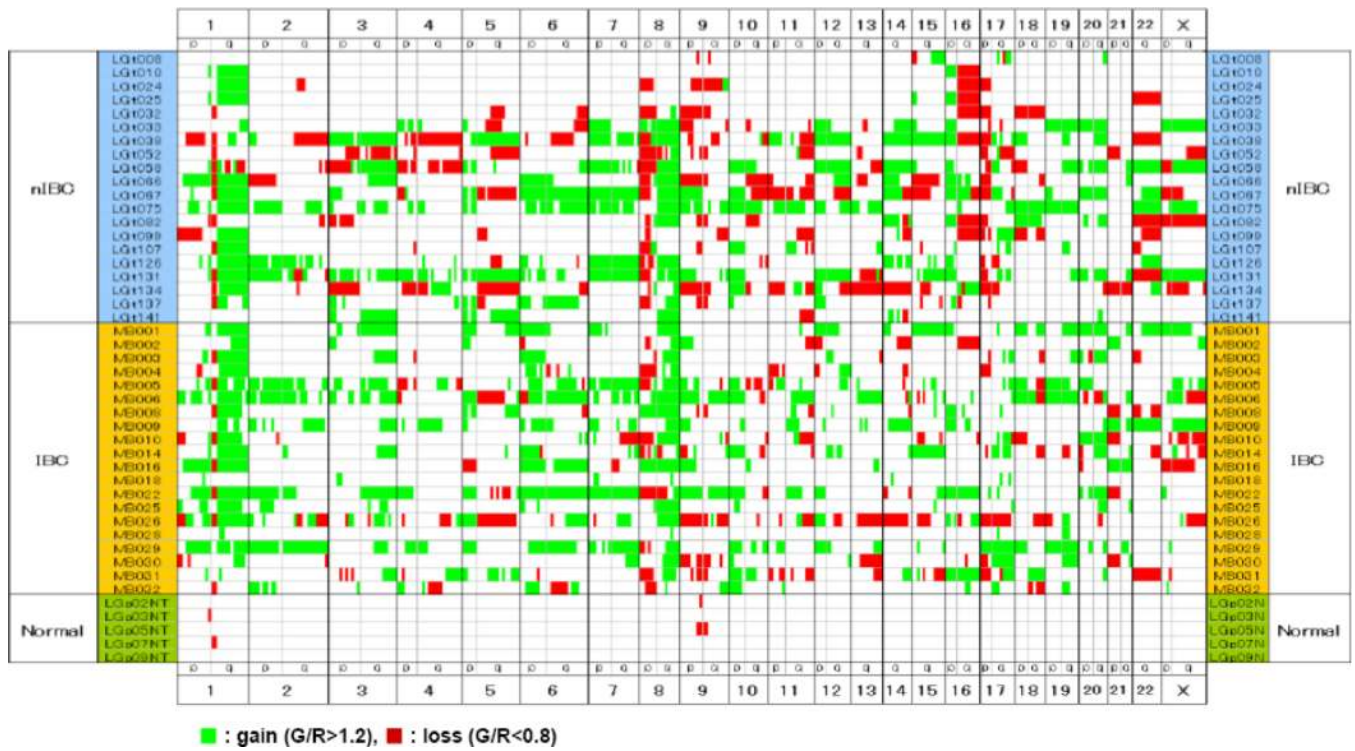
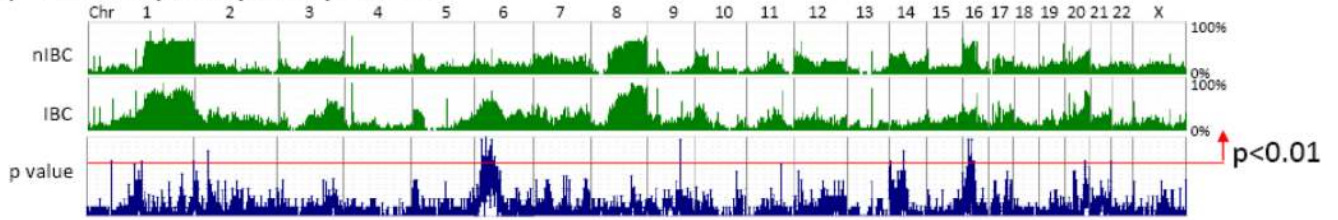


**Figure 4. Overview of genome copy number profiles in all samples**  
 Green indicates increased genome copy number (G/R > 1.2) and red indicates decreased genome copy number (G/R < 0.8).

## (A) Gain frequency and p-value



## (B) Loss frequency and p-value

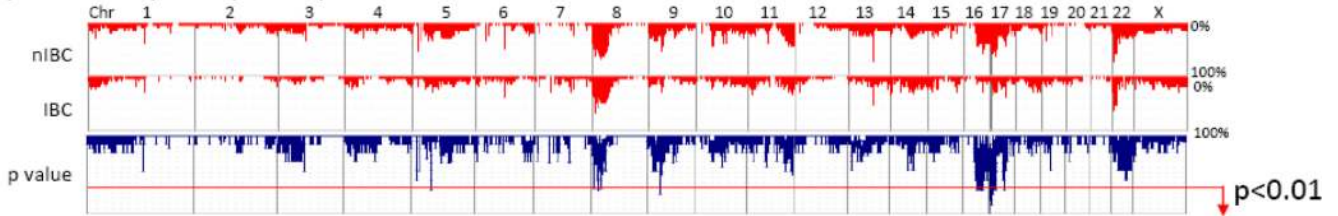


**Figure 5. Frequency of gain/loss in IBC and nIBC and p value between IBC and nIBC**  
 Green indicates increased genome copy number ( $G/R > 1.2$ ) and red indicates decreased genome copy number ( $G/R < 0.8$ ). A. Gain frequency and p-value between IBC and nIBC. B. Loss frequency and p-value between IBC and nIBC. y-axis: negative log of the Fisher's exact test p-value, and red line indicates  $p=0.01$ .

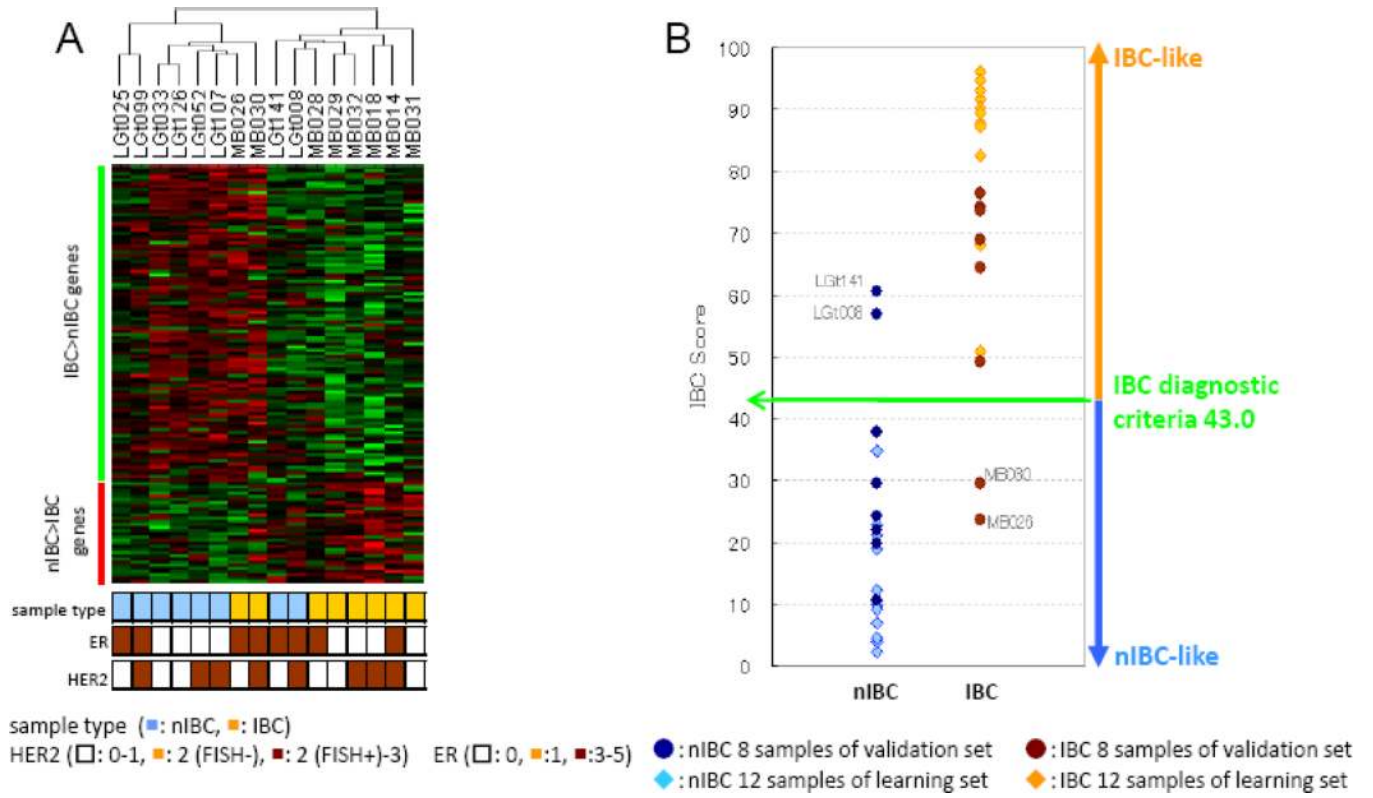


**Figure 6. mRNA validation data**

(A) Unsupervised hierarchical clustering was performed using 132 genes. High relative expression is green, low relative expression is red. Sample type (IBC or nIBC) and ER/HER2 status (based on IHC) of the samples are color-coded as shown. (B) Distribution of the IBC scores of the validation and learning sets.

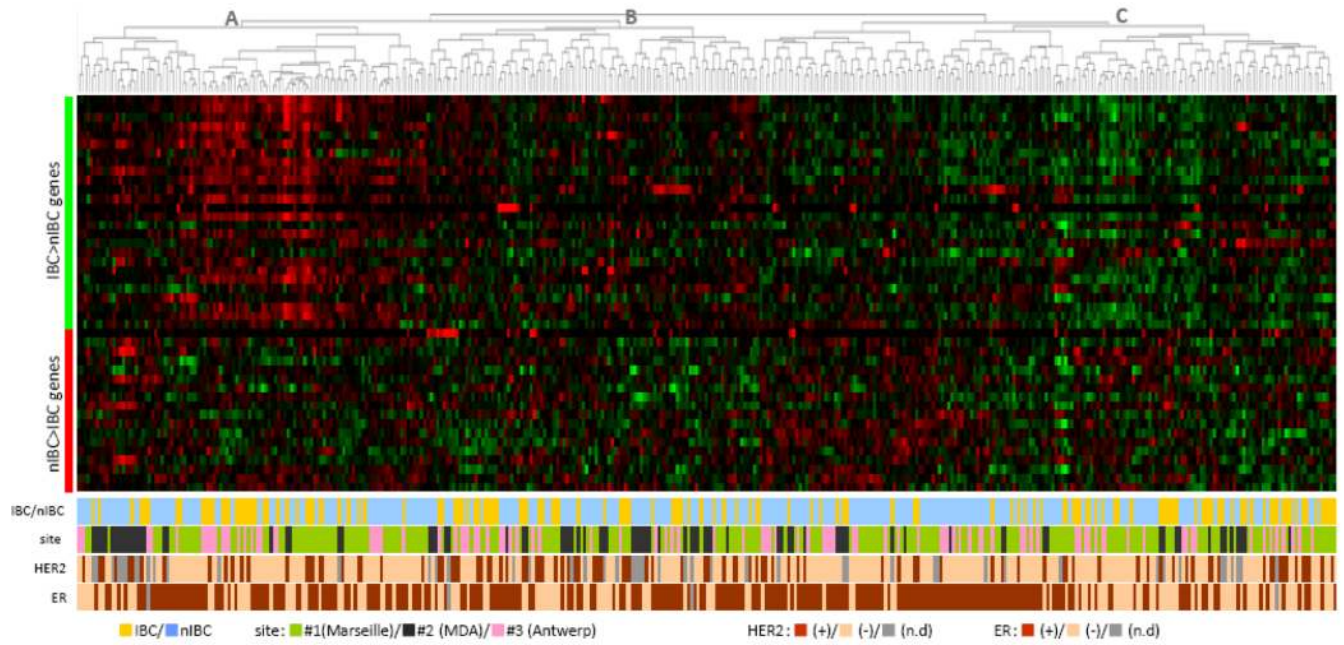
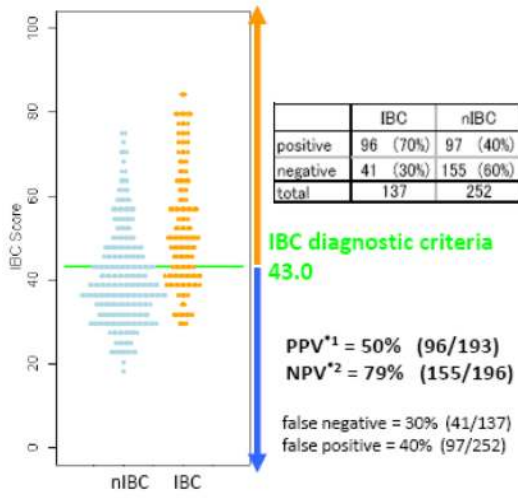


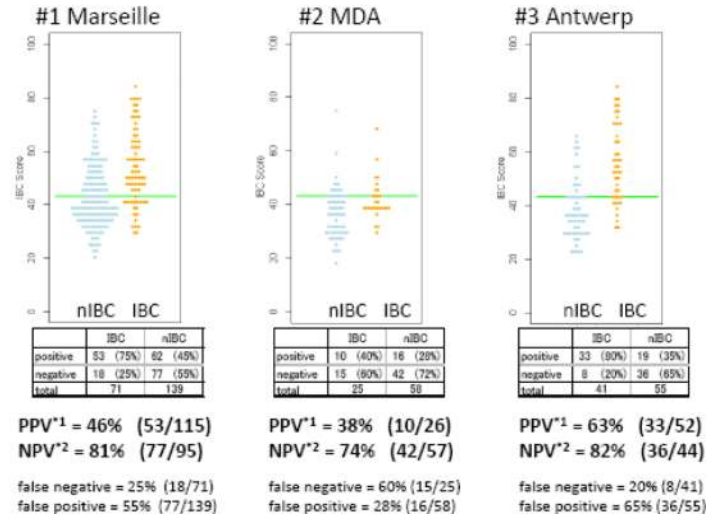
**Figure 7. mRNA clustering analysis of data from IBC consortium institutions**

Clustering analysis was conducted using 44 genes that were in common with the 132 gene set. No IBC enriched cluster was identified.

**(a) all data (389 samples)**

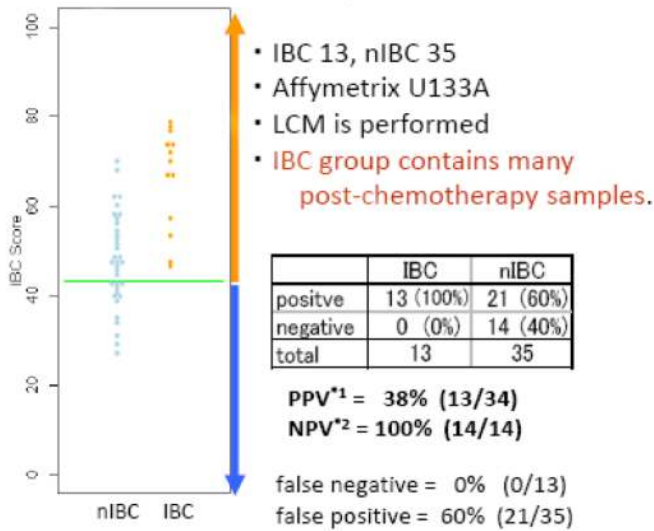
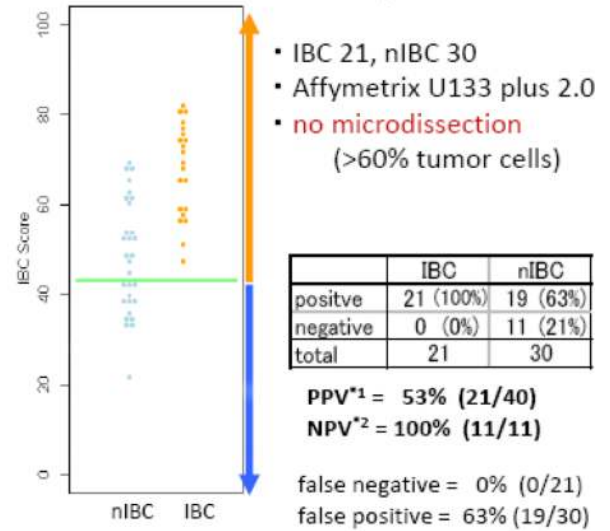


**(b) Each institution**



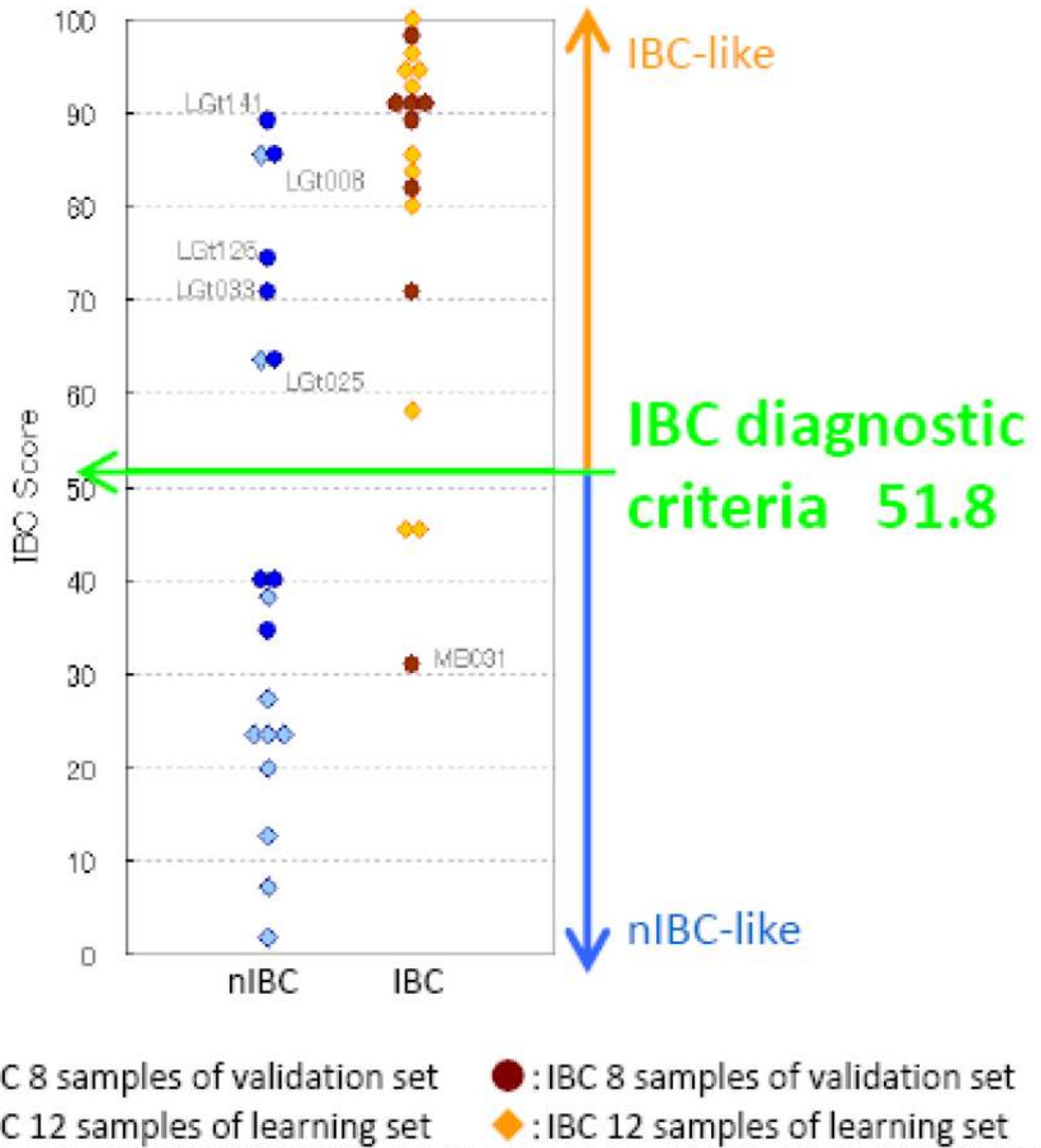
**Figure 8. Distribution of IBC likeness score in consortium data**  
 Distribution of the IBC scores of each sample computed with 44 genes (in common with our 132 genes) in IBC consortium institution data.



**(a) GSE5847**Boersma et al. *Int. J. Cancer* 2008, 122:1324**(b) GSE17907**Sircoulomb et al. *BMC Cancer* 2010, 10:539

<sup>\*1</sup> PPV = positive predictive value, <sup>\*2</sup> NPV = negative predictive value

Figure 9. Distribution of IBC likeness scores in public data sets



**IBC score** = positive BACs / 55 (all BACs) x100

Figure 10. Distribution of the IBC genome copy number based scores of the validation and learning sets

Table 1

## Gene Ontology Function

Term	Count	PValue	Genes
GO:0015671 oxygen transport	3	0.002	HBA1 HBA2 HBB HBD
GO:0007155 cell adhesion	11	0.002	CDH5 PCDHB9 MLLT4 BOC CXCL12 SDK2 FAT2 TEK VWF PCDH17
GO:0022610 biological adhesion	11	0.002	CDH5 PCDHB9 MLLT4 BOC CXCL12 SDK2 FAT2 TEK VWF PCDH17
GO:0015669 gas transport	3	0.003	HBA1 HBA2 HBB HBD
GO:0001525 angiogenesis	5	0.006	CXCL12 ACVRL1 TGFA NOTCHI ENPEP
GO:0001568 blood vessel development	6	0.006	CDH5 CXCL12 ACVRL1 TGFA NOTCHI ENPEP
GO:0001944 vasculature development	6	0.007	CDH5 CXCL12 ACVRL1 TGFA NOTCHI ENPEP
GO:0042060 wound healing	5	0.013	ACVRL1 NOTCHI VWF PROS1 SDC1
GO:0048514 blood vessel morphogenesis	5	0.019	CXCL12 ACVRL1 TGFA NOTCHI ENPEP
GO:0007156 homophilic cell adhesion	4	0.025	CDH5 PCDHB9 FAT2 PCDH17
GO:0016337 cell-cell adhesion	5	0.044	CDH5 PCDHB9 FAT2 TEK PCDH17
Term	Count	PValue	Genes
GO:0032870 cellular response to horm one stimulus	3	0.018	DUSP1 GNG12 FOS

Table 2

Gene expression correlated to genomic change in IBC.

Gene Symbol	Entrez Gene ID	Locus	Description	Genomic Analysis			Expression Analysis				
				r <sup>*1</sup>	BC	nBC	p value*2	amplified	not-amplified	ratio	
1	ZNF184	7738	6p22	zinc finger protein 184	0.84	55%	10%	0.006	328	243	1.35
2	TTRAP	51567	6p22	TRAF and TNF receptor associated protein	0.76	45%	0%	0.001	5505	3414	1.61
3	C6orf89	221477	6p21	chromosome 6 open reading frame 89	0.73	60%	15%	0.008	3109	1891	1.64
4	C6orf62	81688	6p22	chromosome 6 open reading frame 62	0.70	45%	0%	0.001	2744	1765	1.55
5	NFKBL1	4795	6p21	nuclear factor of kappa light polypeptide gene enhancer in B-cells inhibitor-like 1	0.67	45%	5%	0.008	188	130	1.45
6	C6orf47	57827	6p21	chromosome 6 open reading frame 47	0.67	45%	5%	0.008	1391	860	1.62
7	BAT3	7917	6p21	HLA-B associated transcript 3	0.66	45%	5%	0.008	6394	4702	1.36
8	MDC1	9656	6p21	mediator of DNA damage checkpoint 1	0.64	40%	0%	0.003	2188	1441	1.52
9	CSNK2B	1460	6p21	casein kinase 2, beta polypeptide	0.64	50%	5%	0.003	15019	10925	1.37
10	EHMT2	10919	6p21	euchromatic histone-lysine N-methyltransferase 2	0.64	50%	5%	0.003	1184	803	1.48
11	ABCF1	23	6p21	ATP-binding cassette, sub-family F (GCN20), member 1	0.63	55%	10%	0.006	3441	2375	1.45
12	MTCH1	23787	6p21	mitochondrial carrier homolog 1 (C. elegans)	0.61	60%	15%	0.008	64734	47211	1.37
13	TUBB	203068	6p21	tubulin, beta	0.60	40%	0%	0.003	3338	2389	1.40
14	OR2B6	26212	6p22	olfactory receptor, family 2, subfamily B, member 6	0.60	35%	0%	0.008	24	16	1.49
15	ZNF217	7764	20q13	zinc finger protein 217	0.60	60%	15%	0.008	3223	1779	1.81

**Table 3**

mRNA IBC assessment in IBC consortium data from three institutions

Samples	3 institution integrated data									MD Anderson & LG	
	ALL		#1 Marseille		#2 MD Anderson		#3 Antwerp				
	Microdissection % tumor	no microdissection (60~80%)		(surgical biopsy & tissue) (no microdissection) (> 60%)		Fine Needle Aspiration no microdissection (60~80%)		(tissue) (no microdissection)		Core Biopsy & tissue microdissected > 90%	
		BC	nBC	BC	nBC	BC	nBC	BC	nBC	BC	nBC
No. of Samples		137	252	71	139	25	58	41	55	20	20
ER status	ER-positive	55 (41%)	86 (34%)	32 (45%)	42 (30%)	6 (24%)	32 (54%)	17 (44%)	12 (22%)	13 (65%)	13 (65%)
	ER-negative	80 (59%)	164 (66%)	39 (55%)	97 (70%)	19 (76%)	24 (46%)	22 (56%)	43 (78%)	7 (35%)	7 (35%)
	p-value	p=0.22		p<0.05		p<0.05		p<0.05		no significance	
HER2 status	HER2-Amplified	72 (30%)	172 (70%)	34 (48%)	111 (80%)	11 (79%)	16 (55%)	27 (69%)	45 (82%)	8 (40%)	8 (40%)
	HER2-normal	52 (57%)	40 (43%)	37 (52%)	17 (20%)	3 (21%)	13 (45%)	12 (31%)	10 (18%)	12 (60%)	12 (60%)
	p-value	p<0.01		p<0.01		p=0.187		p=0.22		no significance	
cStage	I	0	65 (26%)	0	48 (36%)	0	0	0	17 (31%)	0	13 (65%)
	II	0	97 (39%)	0	75 (56%)	0	0	0	22 (40%)	0	7 (35%)
	III	83 (75%)	66 (27%)	36 (77%)	9 (7%)	21 (84%)	45 (78%)	26 (67%)	12 (22%)	20 (100%)	0
	IV	28 (25%)	20 (8%)	11 (23%)	3 (2%)	4 (16%)	13 (22%)	13 (33%)	4 (7%)	0	0
cT Stage	T0	0	13 (5%)	0	12 (9%)	0	1 (2%)	0	0	0	0
	T1	0	64 (26%)	0	41 (30%)	0	0	0	23 (42%)	0	13 (65%)
	T2	0	90 (36%)	0	68 (50%)	0	0	0	22 (40%)	0	7 (35%)
	T3	0	21 (8%)	0	13 (10%)	0	0	0	8 (15%)	0	0
	T4	137 (100%)	61 (24%)	71 (100%)	2 (1%)	25 (100%)	57 (98%)	41 (100%)	2 (4%)	20 (100%)	0
Platform		Affymetrix 7056 gene 1 color		Affymetrix 7056 gene 1 color		Affymetrix 7056 gene 1 color		Affymetrix 7056 gene 1 color		Agilent 44K ~20,000 (genes) 1 color	